



**HAL**  
open science

## **A step forward: hydrogen production on cobalt molybdenum sulfide electrocatalyst in anion exchange membrane water electrolyzer**

Carlos V. M. Inocêncio, Frederic Fouda-Onana, Julie Rousseau, Nadia Guignard, Teko Napporn, Cláudia Morais, Boniface Kokoh

### ► To cite this version:

Carlos V. M. Inocêncio, Frederic Fouda-Onana, Julie Rousseau, Nadia Guignard, Teko Napporn, et al.. A step forward: hydrogen production on cobalt molybdenum sulfide electrocatalyst in anion exchange membrane water electrolyzer. ACS Applied Energy Materials, 2022, 5 (9), pp.10396-10401. 10.1021/acsaem.2c02270 . cea-03822512

**HAL Id: cea-03822512**

**<https://cea.hal.science/cea-03822512>**

Submitted on 14 Nov 2023

**HAL** is a multi-disciplinary open access archive for the deposit and dissemination of scientific research documents, whether they are published or not. The documents may come from teaching and research institutions in France or abroad, or from public or private research centers.

L'archive ouverte pluridisciplinaire **HAL**, est destinée au dépôt et à la diffusion de documents scientifiques de niveau recherche, publiés ou non, émanant des établissements d'enseignement et de recherche français ou étrangers, des laboratoires publics ou privés.

**A step forward: Hydrogen production on cobalt molybdenum sulfide  
electrocatalyst in anion exchange membrane water electrolyzer**

Carlos V. M. Inocêncio<sup>1</sup>, Frédéric Fouda-Onana<sup>2</sup>, Julie Rousseau<sup>1</sup>, Nadia Guignard<sup>1</sup>, Teko

Napporn<sup>1</sup>, Cláudia Morais<sup>1\*</sup>, K. Boniface Kokoh<sup>1\*</sup>

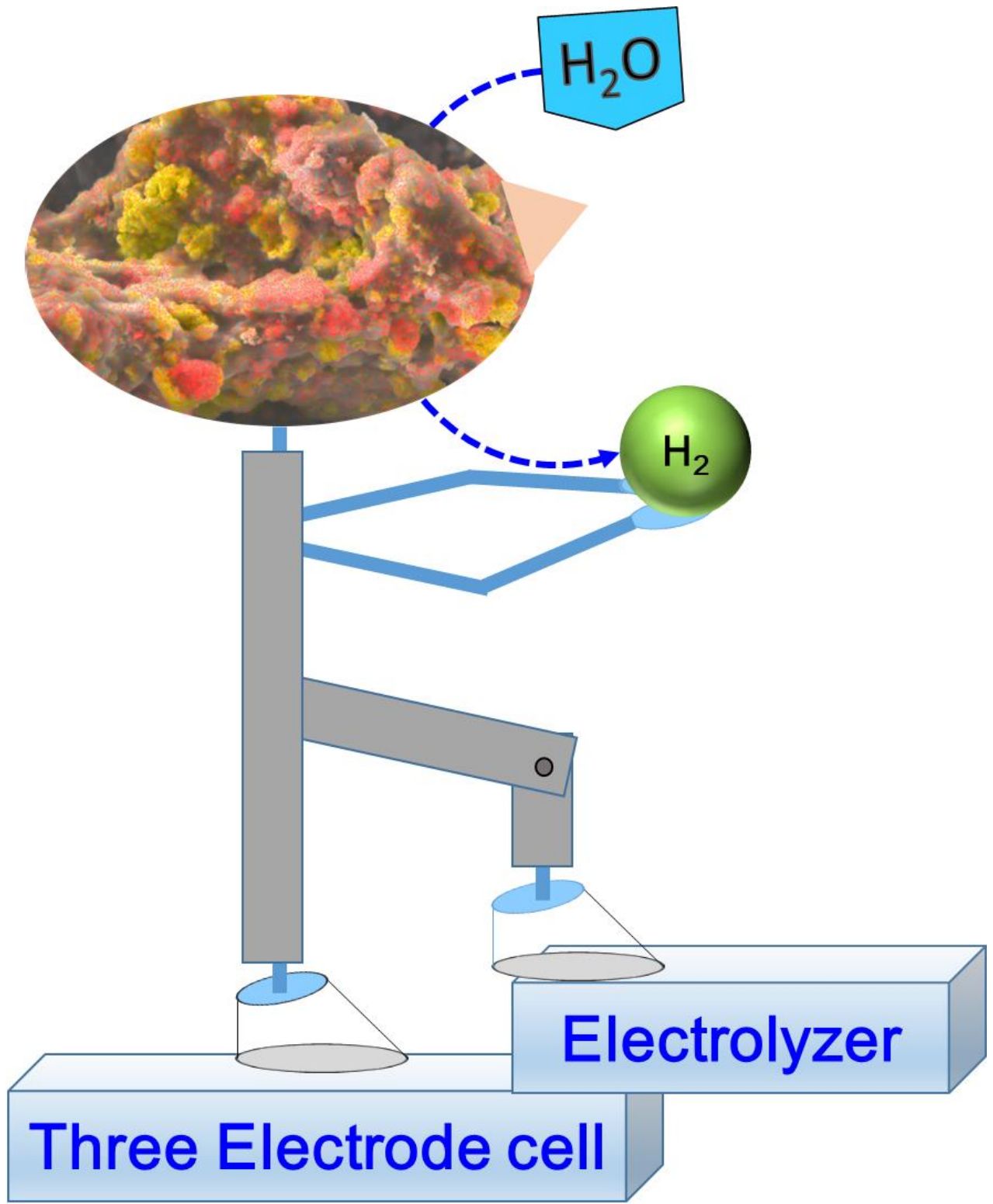
<sup>1</sup> Université de Poitiers, IC2MP, UMR-CNRS 7285, 4, rue Michel Brunet, B27, TSA 51106, 86073

Poitiers cedex 09, France.

<sup>2</sup> Université Grenoble Alpes, CEA, 17 avenue des Martyrs, Grenoble, F-38000, France

## **Abstract**

Cobalt molybdenum sulfide ( $\text{Co}_{0.5}\text{Mo}_{0.5}\text{S}_x$ ) was evaluated, as alternative cathode catalyst for hydrogen large scale production in an anion exchange membrane water electrolyzer (AEMWE). Performance testing in a  $\text{Co}_{0.5}\text{Mo}_{0.5}\text{S}_x//\text{Ir}$  single cell fed with  $0.1 \text{ mol L}^{-1}$  KOH exhibited the best activity reported to date for transition metal sulfide cathodes in alkaline media. The aforementioned cell presented good stability during 40 h of operation at 2 V, besides to have most of its current density degradation recovered in the beginning of subsequent 10 h interval.



H<sub>2</sub> production on Co<sub>0.5</sub>Mo<sub>0.5</sub>S<sub>x</sub> as cathode of an Electrolyzer

Hydrogen ( $H_2$ ) is expected to play an important role to enable energy transition to clean energy since its oxidation leads to the release of energy and only generates water as by-product.<sup>1</sup> In contrast, most of industrial hydrogen production still utilizes fossil sources as feedstock.<sup>2-3</sup> Therefore, to really achieve the goal of carbon footprint decrease, while hydrogen acts as energy carrier, alternative processes for its production must be further developed. Water electrolysis emerges as the most promising process for this purpose once it demands energy, which can be derived from renewable sources, e.g. wind and solar, to split water towards high purity hydrogen and oxygen in the cathode and anode compartments, respectively.<sup>1, 4-5</sup> Water electrolyzers may exist in several configurations. Specifically, the one known as anion exchange membrane water electrolyzer (AEMWE), though still in research stages, has the potential to operate at high current densities, besides to avoid the use of platinum-group metals (PGM) catalysts;<sup>6</sup> both very relevant features. Hence, the goal of this work is to propose new electrocatalysts to be applied as cathode in AEMWE.

It was reported, by theoretical calculations and experimental studies, that transition metal sulfides (TMS) are effective catalysts for the hydrogen evolution reaction (HER) when the sulfur atoms are present at the edge of the structure.<sup>7</sup> Hence this group (Mo, Co), based sulfides, was synthesized by a methodology described recently.<sup>8</sup>

It is presented herein the results obtained for monometallic and bimetallic cobalt- and molybdenum-based sulfides. The main phases obtained for monometallic catalysts were disulfides, i.e.,  $CoS_2$  and  $2H-MoS_2$ , which is in accordance with the stoichiometry applied during their syntheses. The bimetallic sulfide consisted mostly of  $CoS$  and  $MoS_2$  hexagonal phases, though its surface characterization also unveiled the existence of sulfide structure containing both cobalt and molybdenum. Furthermore, it was noticed that both molybdenum disulfide phases aforesaid for Mo-containing catalysts were defect-rich; this feature was revealed to be very relevant for the enhancement of  $MoS_2$  activity towards the hydrogen evolution reaction (HER).<sup>9</sup> A deeper investigation, aided by XRD, Raman spectroscopy, TEM, HAADF-STEM and XPS, and interpretation of physico-chemical nature of the electrocatalysts reported hither may be found in a previous publication.<sup>8</sup>

In addition, elemental composition of  $Co_{0.5}Mo_{0.5}S_x$  was investigated by ICP-OES and XPS analyses, mainly to ascertain if Co:Mo atomic ratio followed the stoichiometry applied in the synthesis; the results are summarized in Table 1. One may notice that, according to ICP-

OES data, Co:Mo ratio agreed with targeted values, *i.e.*, the equimolarity of metals was preserved. Likewise, S:Mo ratio around 3 also indicated a coherence in the coexistence of CoS and MoS<sub>2</sub> phases. Different proportionality was obtained by XPS quantitative analysis, but nevertheless the results are not necessarily antagonistic as XPS results are restricted to its surface while ICP-OES provides a global information of the sample. Therefore, it may be stated that Co<sub>0.5</sub>Mo<sub>0.5</sub>S<sub>x</sub> surface is poorer in cobalt than its bulk. The former statement was confirmed by Raman spectroscopy also restricted to surface, albeit it can probe deeper regions of sample than XPS. Indeed, in the catalyst's Raman spectrum (**Figure S1**) bands associated with tertiary sulfides were identified but no band related to CoS<sub>x</sub> species could be detected, although CoS phase was clearly identified in Co<sub>0.5</sub>Mo<sub>0.5</sub>S<sub>x</sub>.

**Table 1.** Atomic ratio of elements in Co<sub>0.5</sub>Mo<sub>0.5</sub>S<sub>x</sub>, normalized with the molybdenum amount obtained by ICP-OES and XPS techniques.

Element ratio*	ICP-OES	XPS
$\frac{n_{\text{Co}}}{n_{\text{Mo}}}$	1.09	0.15
$\frac{n_{\text{S}}}{n_{\text{Mo}}}$	3.07	1.74

\*n<sub>x</sub> = quantity, in mol, of element "X".

The electrocatalysts' performance for HER was firstly evaluated in a three-electrode configuration at room temperature; it was used a homemade cell produced with Kel-F® polymer to avoid Pyrex glass cell corrosion in alkaline medium. Glassy carbon slab and Hg/HgO/HO<sup>-</sup> were used as counter and reference electrodes, respectively, whilst rotating disk electrode (RDE) containing a glassy carbon substrate, onto which the cathode catalyst was deposited, was employed as working electrode. After a simple conversion, results were plotted in potential referenced by reversible hydrogen electrode (RHE); to do so, reference electrode calibration was accomplished. Further details concerning the cell configuration, ink preparation and reference calibration are provided in the **Supporting Information**.

Polarization curves (**Figure 1**) were obtained by LSV analysis in N<sub>2</sub>-saturated 1 M KOH at 10 mV s<sup>-1</sup> and 1,600 rpm. Molybdenum sulfide exhibited better HER performance than cobalt sulfide in all the applied potential range. Indeed, molybdenum sulfide has been pointed out as promising HER catalyst by theoretical and experimental studies over the last

two decades.<sup>7, 10-11</sup> However, its activity is reduced once acidic electrolytes are replaced by alkaline ones as a result of its poor water dissociation ability as well as the strong adsorption of generated hydroxyl to its surface.<sup>12</sup> Nonetheless, these characteristics may be tuned by the incorporation of Co-based species to derive a catalyst with superior activity.<sup>12-13</sup> The synergistic effect existing in the bimetallic sulfide is highlighted in the polarization curve (**Figure 1**) as it exhibits less negative onset potential, in addition to generating more than twice current density than monometallic sulfides at -0.56 V vs RHE. To reach 10 mA cm<sup>-2</sup> the overpotential was 181 mV, which set Co<sub>0.5</sub>Mo<sub>0.5</sub>S<sub>x</sub> among the best electrocatalysts for HER in alkaline medium, especially the unsupported ones. Different Co:Mo ratios were previously tested and the equimolar one showed the best result.<sup>8</sup>

Due to the promising character of Co<sub>0.5</sub>Mo<sub>0.5</sub>S<sub>x</sub> as earth-abundant cathode for water electrolysis, it was further tested in a AEMWE configuration. The activity of monometallic sulfides was also investigated to evaluate the relevance of the bimetallic composition. Sustainion® X37-50 Grade RT (Dioxide Material™) and Ir black (Sigma-Aldrich), with mass loading of about 2 mg cm<sup>-2</sup>, were used as anion exchange membrane and anode for all measurements. Despite iridium is a scarce element and a noble metal, it has been widely used in water electrolyzers<sup>14-16</sup> and, therefore, it plays a role herein as reference anode to evaluate cathode's activity, the main goal of this paper.

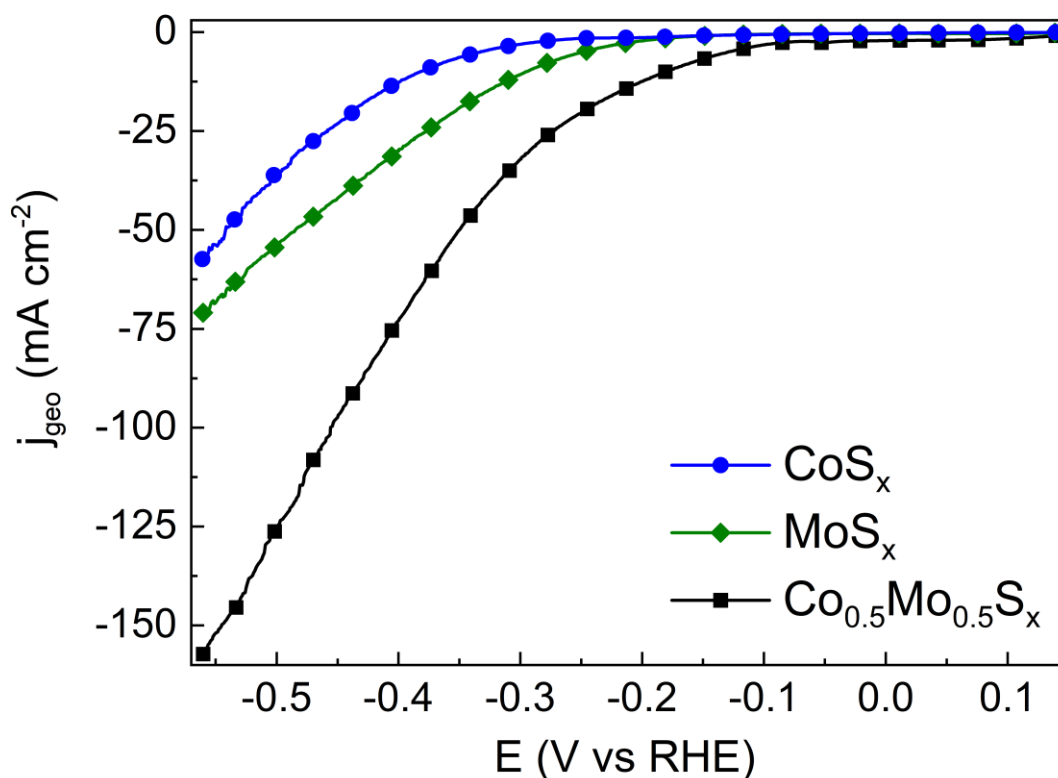


**Figure 1.** Polarization curves acquired with RDE system (1,600 rpm) in N<sub>2</sub>-saturated 1 mol L<sup>-1</sup> KOH at 10 mV s<sup>-1</sup>, and room temperature.

Polarization curves, presented in **Figure 2**, were recorded at 50 °C by applying a 10 mV s<sup>-1</sup> scan rate in an AEMWE cell, 1.8 cm<sup>2</sup> electrodes' geometrical surface area, fed with 2 mL min<sup>-1</sup> of 0.1 M KOH. More experimental details are given in **Supporting Information**. At low current density, between 0 and 0.1 A cm<sup>-2</sup>, CoS<sub>x</sub> presented the highest activity. It may be related to its superior water dissociation ability when compared to Mo-based sulfides, though the same trend was not verified in the three-electrode cell configuration. Conversely, in the region where polarization curves assume a linear profile, i.e., at high current densities, CoS<sub>x</sub> becomes less active than molybdenum-based catalysts. In fact, polarization profiles of MoS<sub>x</sub> and Co<sub>0.5</sub>Mo<sub>0.5</sub>S<sub>x</sub> are very similar and the major difference comes from the onset voltage of water splitting; lower for the bimetallic sulfide. While the similarity is prone to be a consequence of Co<sub>0.5</sub>Mo<sub>0.5</sub>S<sub>x</sub> surface being rich in molybdenum, the difference probably arises from faster water dissociation promoted by cobalt species. The cell composed by Co<sub>0.5</sub>Mo<sub>0.5</sub>S<sub>x</sub> and Ir black as cathode and anode (Co<sub>0.5</sub>Mo<sub>0.5</sub>S<sub>x</sub>//Ir), respectively, achieved *ca.* 1.2 A cm<sup>-2</sup> at 2 V; a current density about 28 % higher than the one obtained once Co<sub>0.5</sub>Mo<sub>0.5</sub>S<sub>x</sub>



was replaced by MoS<sub>x</sub>. A comparison of activity normalized by cathode mass can be verified in Figure S5.

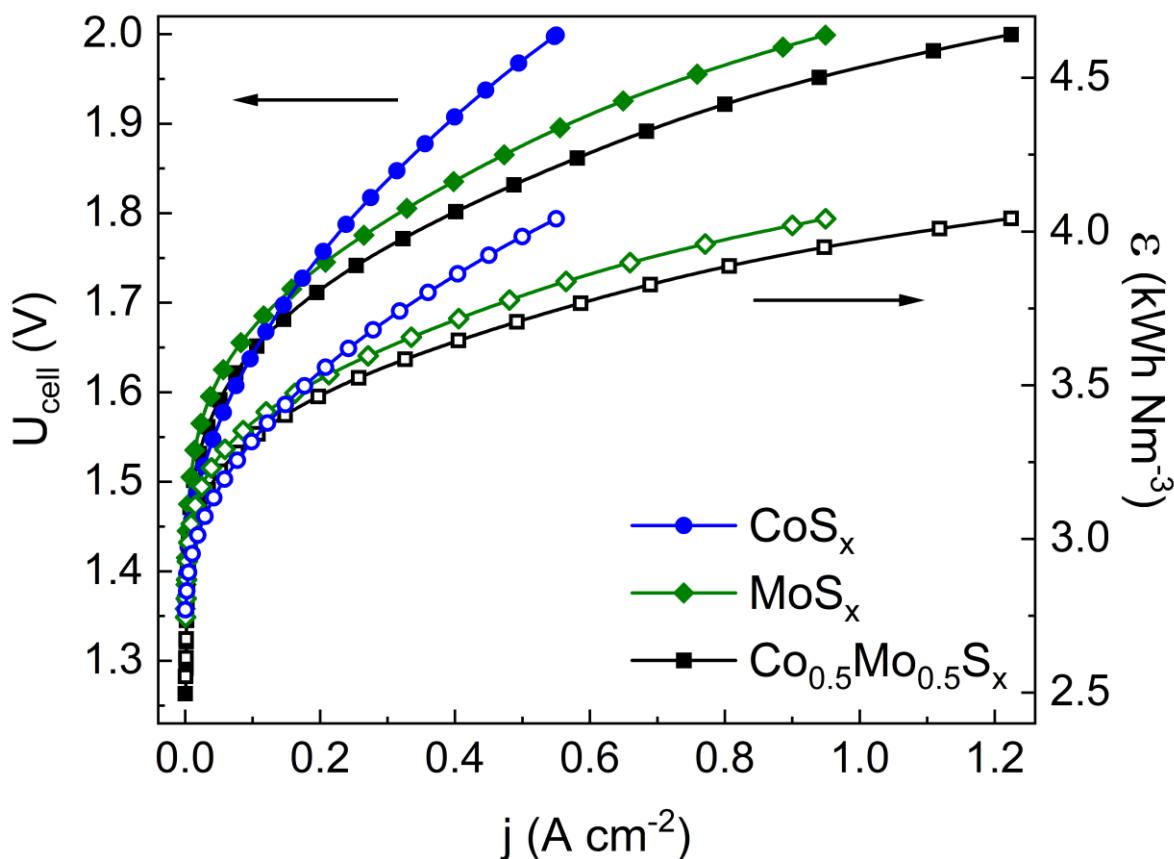


**Figure 2.** Polarization (left) and specific energy consumption (right) curves obtained from analysis in AEMWE device fed by 0.1 M KOH. Ir black and Sustainion® X37-50 were applied as anode catalyst and membrane, respectively, for all measurements.

To the best of our knowledge, there are only two articles reporting the use of TMS materials as cathode of AEMWE, specifically Co<sup>15, 17</sup> and Ni-based<sup>15</sup> sulfides. At 2 V, Guo *et al.*<sup>15</sup> reported a current density about 0.5 A cm<sup>-2</sup> for Ni-Co-S//IrO<sub>2</sub> configuration operated at 50 °C, while the value obtained by Park *et al.*<sup>17</sup> was of 0.431 A cm<sup>-2</sup> for Co<sub>3</sub>S<sub>4</sub>//Cu<sub>0.81</sub>Co<sub>2.19</sub>O<sub>4</sub> cell; both systems were fed with 1 M KOH. Both results revealed performance lower than those measured in this work with a KOH concentration ten-fold diluted, i.e., Co<sub>0.5</sub>Mo<sub>0.5</sub>S<sub>x</sub> (or MoS<sub>x</sub>)//Ir systems. Although different metal sulfides have been investigated as HER catalysts, molybdenum sulfide is the most representative one and has been widely researched as PGM-free alternative catalyst during the last three decades.<sup>1</sup> Despite that, the

application of Mo-based sulfides electrocatalysts in the cathodic compartment of AEMWE device is reported for the first time herein.

Ni-containing materials for AEMWE were also investigated using 0.1 M KOH concentration for increasing the ionic conductivity. Under the same conditions with ours (50 °C and Ir as anode), current densities of 0.5 and 1 A cm<sup>-2</sup> at 2 V were obtained with NiMo/C and NiCu MMO/C cathodes, respectively.<sup>14, 16</sup> Interestingly, both cells were also tested with higher electrolytic concentration (1 M KOH), which led to best performance. Although the increase of electrolyte concentration boosts cell performance, it brings technological disadvantages and, therefore, the goal is, in fact, to reduce it until the technology reaches maturity as verified for proton exchange membrane water electrolyzers (PEMWE), which are only fed with water.<sup>6</sup> So far, most studies in AEMWE operate with 1 M KOH feeding<sup>18</sup>, making the result reported herein even more relevant since an excellent cell performance was obtained with KOH concentration ten-fold lower than those commonly reported. Table 2 summarizes the performance of mentioned AEMWE cells.

**Table 2.** Performance comparison of different AEMWE cells at 2 V and operated at 50 °C.

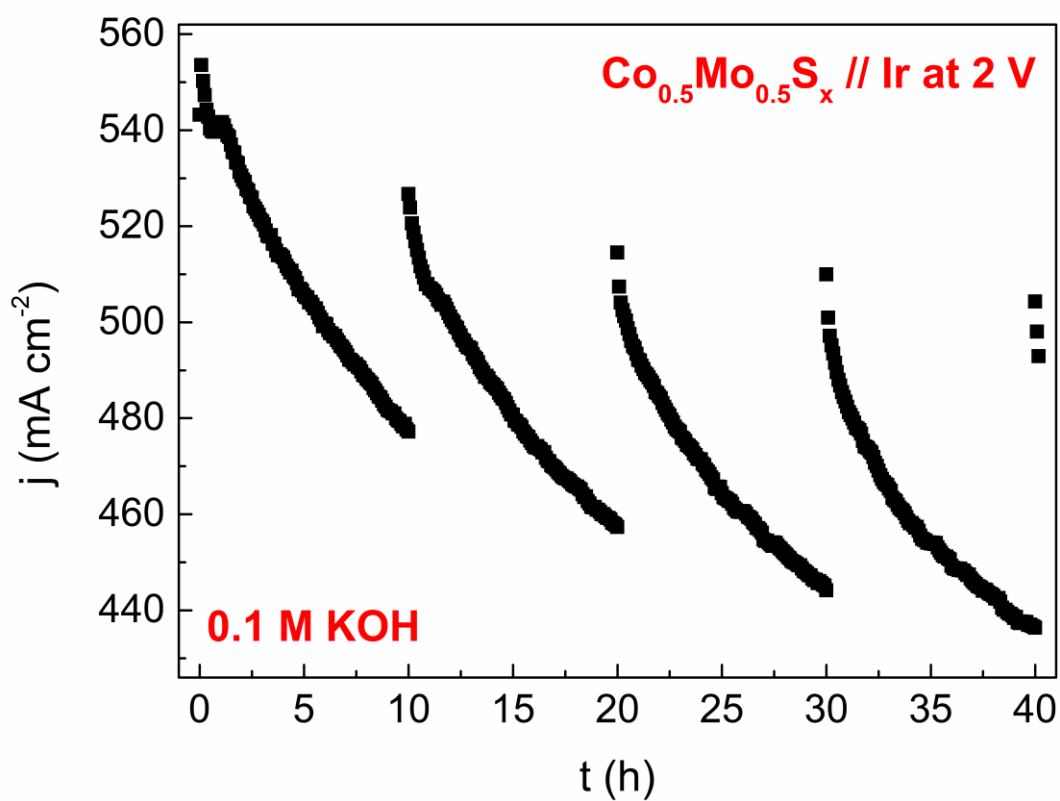
Cathode	Anode	j (A cm <sup>-2</sup> )	KOH concentration (mol L <sup>-1</sup> )	Reference
CoS <sub>x</sub>	Ir	0.55	0.1	This work
MoS <sub>x</sub>	Ir	0.95	0.1	This work
Co <sub>0.5</sub> Mo <sub>0.5</sub> S <sub>x</sub>	Ir	1.22	0.1	This work
NiCu MMO/C	Ir	1.0	0.1	14
Ni-Co-S	IrO <sub>2</sub>	0.5	1.0	15
NiMo/C	Ir	0.5	0.1	16
Co <sub>3</sub> S <sub>4</sub>	Cu <sub>0.81</sub> Co <sub>2.19</sub> O <sub>4</sub>	0.431	1.0	17

Figure 2 also reports values of specific energy consumption derived from polarization curves. Genuinely, such parameter varies with cell voltage ( $U_{\text{cell}}$ ), however, current density has linear relation to quantity of hydrogen produced, assuming 100 % of faradaic efficiency, and the function  $U_{\text{cell}}(j)$  depends on the applied catalyst. Therefore, by assuming an operational consumption of 4 kWh per Nm<sup>3</sup> of H<sub>2</sub>, for example, the use of Co<sub>0.5</sub>Mo<sub>0.5</sub>S<sub>x</sub> as cathode would result in a H<sub>2</sub> production of about 27 and 112 % higher than MoS<sub>x</sub> and CoS<sub>x</sub>,

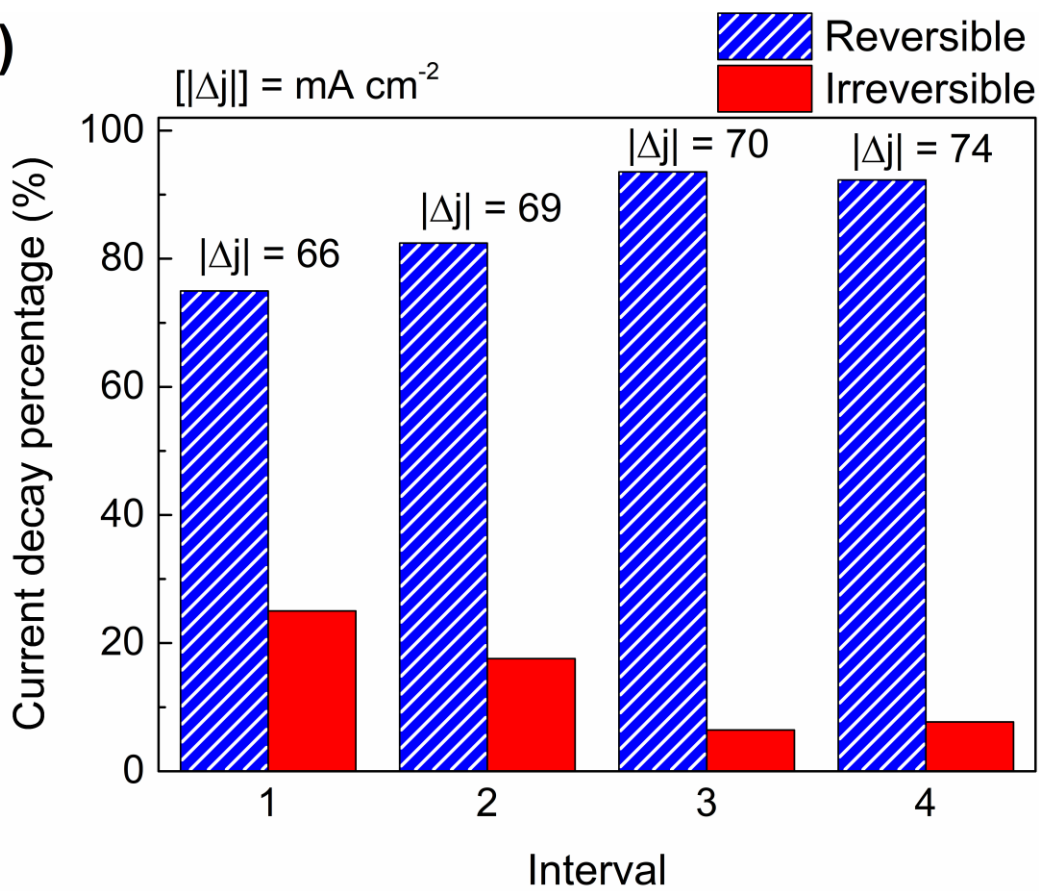
respectively. These differences would certainly have huge impact on hydrogen market price.

Undoubtedly, stability, which is still a bottleneck in AEMWE application,<sup>6</sup> is one of the main aspects to be evaluated in cell performance since the economical suitability of the process depends on its long-term operation. Hence, such feature was evaluated for  $\text{Co}_{0.5}\text{Mo}_{0.5}\text{S}_x//\text{Ir}$  cell by applying 2 V during 40 h. Stability analysis was divided in different steps. The 40 h were uniformly prorated in 4 intervals and polarization analyses at  $5 \text{ mV s}^{-1}$  were performed before stability test and after each interval. Results associated with the 4 intervals are depicted in **Figure 3**, while polarization curves are exhibited in **Figure S6**. In the  $j \times t$  graph (**Figure 3a**), current density decay profile for the  $\text{Co}_{0.5}\text{Mo}_{0.5}\text{S}_x//\text{Ir}$  electrolysis cell can be observed. Most of current density lost during each interval is recovered in the beginning of following one. An investigation of  $\text{Ni-Co-S}//\text{IrO}_2$  stability was performed by Guo *et al.*<sup>15</sup> by applying  $0.4 \text{ A cm}^{-2}$  during 8 h. Regrettably no numerical value nor discussion was provided by the authors and the resultant graph containing a large cell voltage scale makes data analysis difficult. Furthermore,  $\text{IrO}_2$  is deposited onto carbon paper, whereas carbon-based materials are known for being unstable in the anodic compartment due to corrosion issues. The system proposed by Park *et al.*<sup>17</sup> ( $\text{Co}_3\text{S}_4//\text{Cu}_{0.81}\text{Co}_{2.19}\text{O}_4$ ) was submitted to 12 h stability test at  $500 \text{ mA cm}^{-2}$  (applied continuously). Authors reported a good stability once an initial cell voltage of 2 V was registered and about 0.05 V of increase was verified during operation. **Figure 3b** provides further details on current density decay during  $\text{Co}_{0.5}\text{Mo}_{0.5}\text{S}_x//\text{Ir}$  stability testing. As shown, the absolute value of current density decay was, approximately, the same during each interval, about  $70 \text{ mA cm}^{-2}$ . However, part of this decay is reversible from one interval to another, and the reversibility percentage varied in each interval; the percentage of irreversible current decay diminished during the first three intervals and was maintained below 10 % from third interval onwards. Irreversible activity losses are likely related to catalysts degradation, modifications of cell components may not be discarded though. The reversible decay is credited to the blocking of either catalyst surface or fluids channels due to hydrogen bubbles formation; these bubbles can be released once the 2 V application is interrupted to perform the LSV measurement.

a)



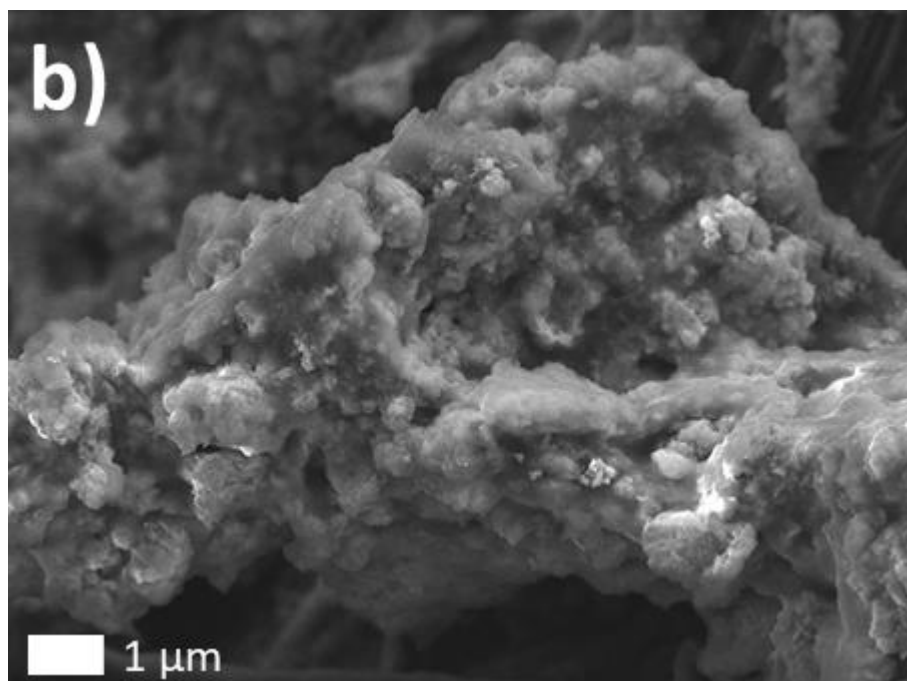
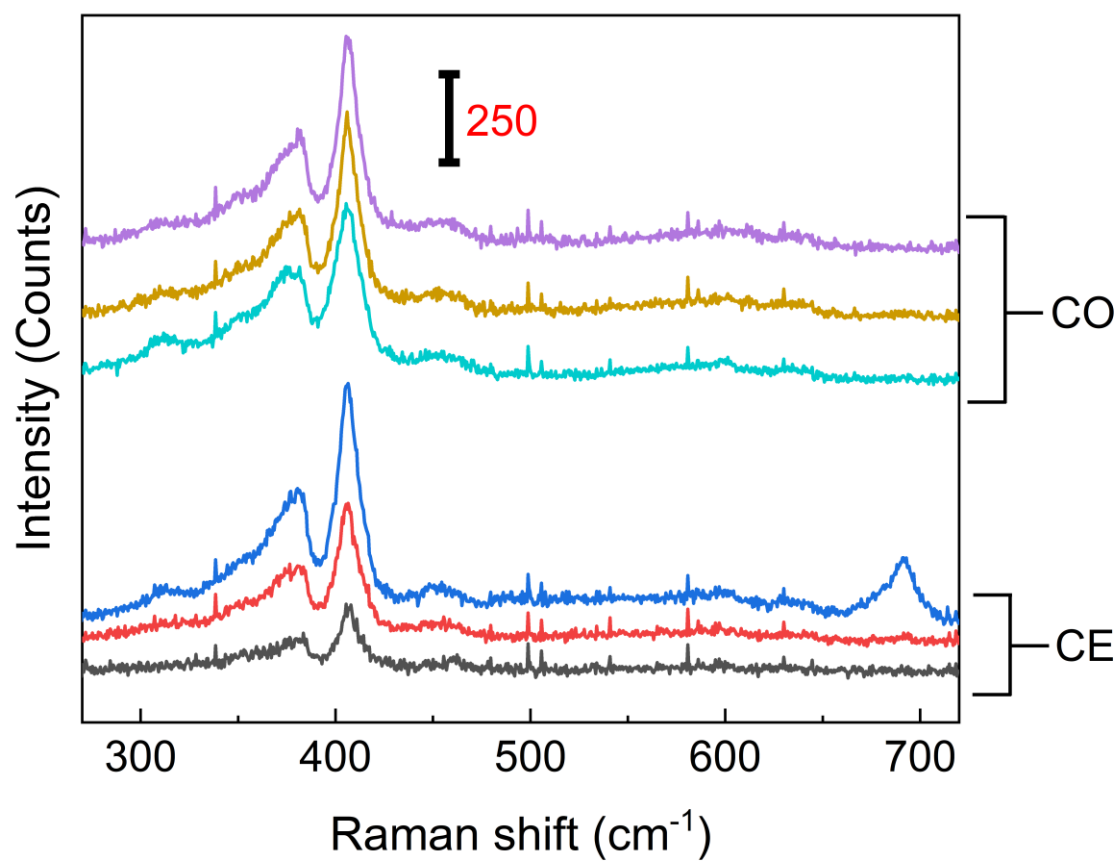
b)

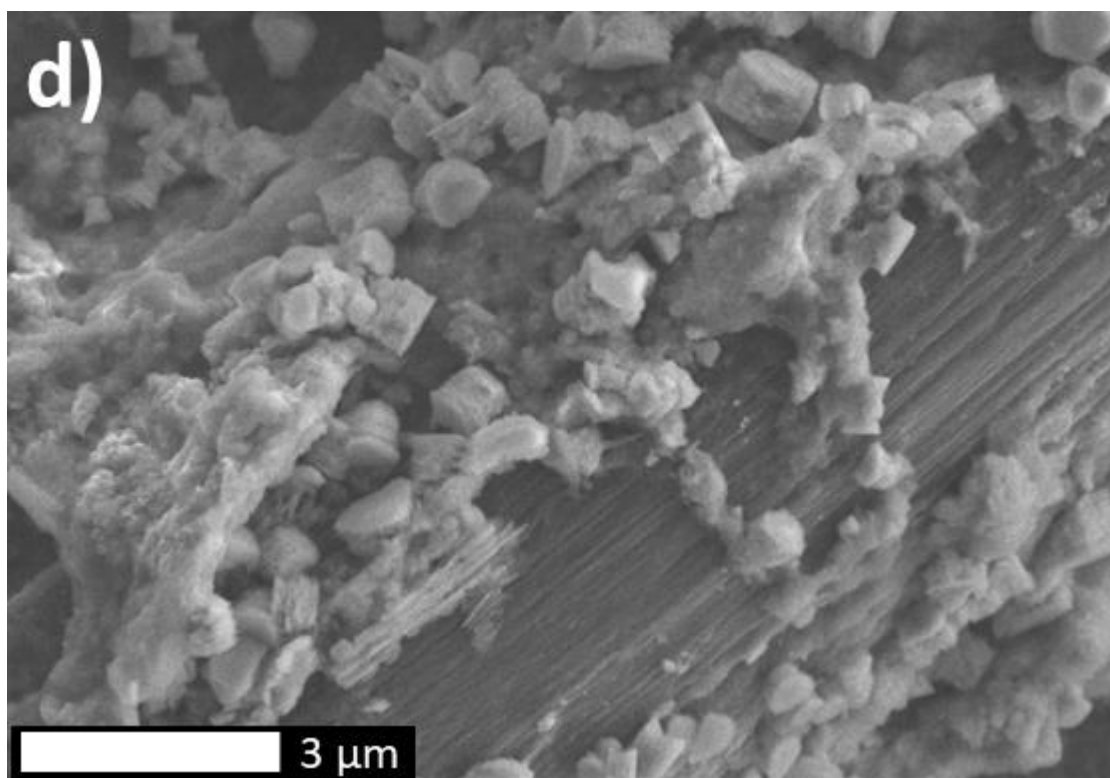
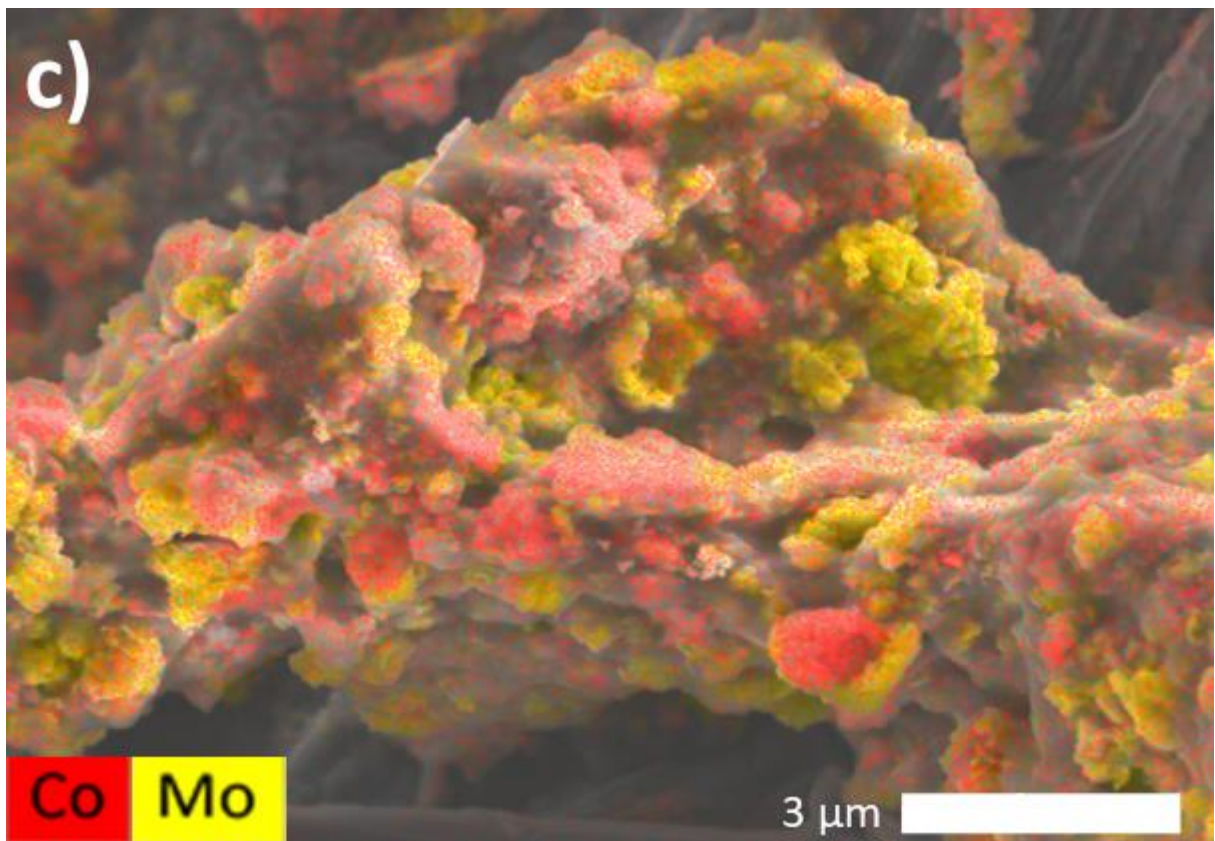


**Figure 3. a)** Chronoamperometry analysis applied to  $\text{Co}_{0.5}\text{Mo}_{0.5}\text{S}_x//\text{Ir}$  system, fed by 0.1 M KOH, at 2 V during 40 h, divided in four intervals of 10 h. **b)** Details of current density decay during stability testing and its reversibility aspect.

Raman spectroscopy and field emission gun scanning electron microscopy (FEG-SEM) analyses of  $\text{Co}_{0.5}\text{Mo}_{0.5}\text{S}_x$ , submitted to 40 h test, were performed to comprehend the irreversible activity decay; results are presented in **Figure 4**. One may see that Raman spectra (**Figure 4a**) were obtained by probing different points of GDE, comprising both center and corner of MEA. Another  $\text{Co}_{0.5}\text{Mo}_{0.5}\text{S}_x//\text{Ir}$  MEA, which was not submitted to any test, was prepared following the same protocol to provide information of  $\text{Co}_{0.5}\text{Mo}_{0.5}\text{S}_x$  GDE before reaction; its Raman spectra are exhibited in **Figure S7**. In general, Raman spectra before and after electrolysis are very similar. It is verified that the characteristic  $E_{12g}$  and  $A_{1g}$  phonon modes<sup>8</sup> of  $\text{MoS}_2$  were preserved during the reaction. The major difference comes from the appearance of a band at  $691\text{ cm}^{-1}$  in one corner spectrum after reaction. This may be associated with the oxidation of cobalt<sup>19</sup> after the MEA was exposed to air. The application of energy dispersive X-ray spectroscopy (EDS) technique during FEG-SEM analyzes provided deeper information (**Figure 4b-e**). **Figures 4c** and **4e** unveiled the occurrence of segregation between cobalt and molybdenum during stability test; **Figure S8** illustrates the good dispersion before reaction. This segregation is likely the irreversible activity loss reason, once superior HER activity of cobalt molybdenum sulfide arises from its bifunctionality.<sup>8</sup>

a)





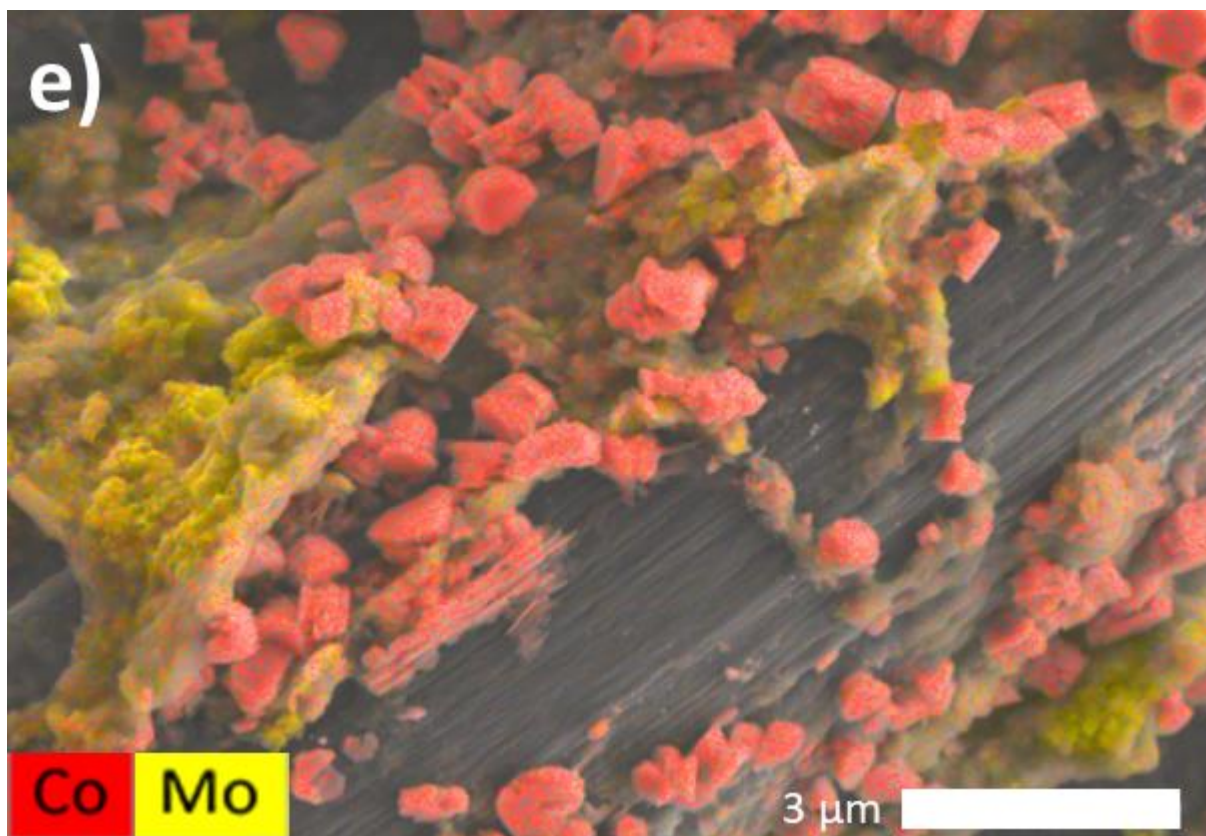


**Figure 4.** a) Raman spectroscopy of aged  $\text{Co}_{0.5}\text{Mo}_{0.5}\text{S}_x$  applied to different points of the GDE. “CO” and “CE” indicate positions at the corner and center of GDE, respectively. b) and d) FEG-SEM images of aged  $\text{Co}_{0.5}\text{Mo}_{0.5}\text{S}_x$  recorded in secondary electron mode. c) and e) Cobalt and molybdenum elemental mapping obtained by EDS technique.

In summary, the  $\text{Co}_{0.5}\text{Mo}_{0.5}\text{S}_x//\text{Ir}$  cell delivered  $1.22 \text{ A cm}^{-2}$  at 2 V in LSV analysis, a value higher than any other TMS cathode. This cell also showed good stability during 40 h of operation at 2 V with current density degradation of ca. 1.4 %/h. Noteworthy, most of such degradation could be recovered by releasing the bubbles from the electrolyzer during a linear sweep polarization; 75 % was recovered after the first ten hours, while from 30 h onwards this recovery surpassed 90 %. FEG-SEM technique demonstrated that the small irreversible activity loss arose from cobalt segregation during the HER process. Results presented herein become even more relevant when considering that AEMWE cell was fed with 0.1 M KOH in electrochemical analyzes, ten times lower than usually applied in the literature.

## ASSOCIATED CONTENT

### Supporting Information



Synthesis method, electrochemical characterizations, experimental set-up of water electrolysis, postmortem characterizations of the MEA

## **AUTHOR INFORMATION**

Corresponding Authors

\*E-mail: boniface.kokoh@univ-poitiers.fr

\*E-mail: claudia.gomes.de.morais@univ-poitiers.fr

## **ORCID**

Carlos V. M. Inocêncio: 0000-0001-7632-0463

Cláudia Morais: 0000-0003-0096-2122

K. Boniface Kokoh: 0000-0002-5379-7792

Teko W. Napporn: 0000-0003-1506-7139

Frédéric Fouda-Onana: 0000-0002-3878-183X

Julie Rousseau: 0000-0002-9464-2420

Nadia Guignard: 0000-0002-0359-7127

## **AUTHOR CONTRIBUTIONS**

Carlos V. M. Inocêncio: Investigation, Methodology, Writing Original draft.

Frédéric Fouda-Onana: Conceptualization, Methodology, Writing, Review.

Julie Rousseau: Methodology, Investigation, Review

Nadia Guignard: Methodology, Investigation, Review

Teko W. Napporn: Conceptualization, Supervision, Writing, Review.

Cláudia Morais: Conceptualization, Supervision, Writing, Review.

K. Boniface Kokoh: Conceptualization, Supervision, Writing, Review.

All authors have given approval to the final version of the manuscript.

## **Notes**

The authors declare no competing financial interest.

## **ACKNOWLEDGMENTS**

The authors from IC2MP thank the “European Union (ERDF),” the “Region Nouvelle-Aquitaine,” and “Grand Angoulême” for their financial supports.

## REFERENCES

1. Inocêncio, C. V. M.; Holade, Y.; Morais, C.; Kokoh, K. B.; Napporn, T. W., Electrochemical Hydrogen Generation Technology: Challenges in electrodes materials for a Sustainable Energy. *Electrochem. Sci. Adv.* **2022**, e2100206, In Press.
2. Sharma, S.; Ghoshal, S. K., Hydrogen the future transportation fuel: From production to applications. *Renew. Sustain. Energy Rev.* **2015**, *43*, 1151-1158.
3. Holladay, J. D.; Hu, J.; King, D. L.; Wang, Y., An overview of hydrogen production technologies. *Catal. Today* **2009**, *139* (4), 244-260.
4. Lasia, A., Mechanism and kinetics of the hydrogen evolution reaction. *Int. J. Hydrogen Energy* **2019**, *44*, 19484-19518.
5. Anantharaj, S.; Ede, S. R.; Sakthikumar, K.; Karthick, K.; Mishra, S.; Kundu, S., Recent Trends and Perspectives in Electrochemical Water Splitting with an Emphasis on Sulfide, Selenide, and Phosphide Catalysts of Fe, Co, and Ni: A Review. *ACS Catal.* **2016**, *6*, 8069-8097.
6. Santoro, C.; Lavacchi, A.; Mustarelli, P.; Di Noto, V.; Elbaz, L.; Dekel, D. R.; Jaouen, F., What is Next in Anion-Exchange Membrane Water Electrolyzers? Bottlenecks, Benefits, and Future. *ChemSusChem* **2022**, e202200027.
7. Hinnemann, B.; Moses, P. G.; Bonde, J.; Jørgensen, K. P.; Nielsen, J. H.; Horch, S.; Chorkendorff, I.; Nørskov, J. K., Biomimetic Hydrogen Evolution: MoS<sub>2</sub> Nanoparticles as Catalyst for Hydrogen Evolution. *J Am Chem Soc* **2005**, *127* (15), 5308-5309.
8. Inocêncio, C. V. M.; Rousseau, J.; Guignard, N.; Canaff, C.; Morisset, S.; Comminges, C.; Morais, C.; Kokoh, K. B., Taking Advantage of Teamwork: Unsupported Cobalt Molybdenum Sulfide as an Active HER Electrocatalyst in Alkaline Media. *J. Electrochem. Soc.* **2022**, *169* (5), 054524.
9. Anjum, M. A. R.; Jeong, H. Y.; Lee, M. H.; Shin, H. S.; Lee, J. S., Efficient Hydrogen Evolution Reaction Catalysis in Alkaline Media by All-in-One MoS<sub>2</sub> with Multifunctional Active Sites. *Adv. Mater.* **2018**, *30*, 1-9.
10. Kong, D.; Wang, H.; Cha, J. J.; Pasta, M.; Koski, K. J.; Yao, J.; Cui, Y., Synthesis of MoS<sub>2</sub> and MoSe<sub>2</sub> Films with Vertically Aligned Layers. *Nano Lett.* **2013**, *13* (3), 1341-1347.
11. Jaramillo, T. F.; Jørgensen, K. P.; Bonde, J.; Nielsen, J. H.; Horch, S.; Chorkendorff, I., Identification of active edge sites for electrochemical H<sub>2</sub> evolution from MoS<sub>2</sub> nanocatalysts. *Science* **2007**, *317*, 100-102.
12. Zhang, J.; Wang, T.; Liu, P.; Liu, S.; Dong, R.; Zhuang, X.; Chen, M.; Feng, X., Engineering water dissociation sites in MoS<sub>2</sub> nanosheets for accelerated electrocatalytic hydrogen production. *Energy Environ. Sci.* **2016**, *9*, 2789-2793.

13. Mukherji, A.; Bal, R.; Srivastava, R., Understanding the Co : Mo Compositional Modulation and Fe-Interplay in Multicomponent Sulfide Electrocatalysts for Oxygen and Hydrogen Evolution Reactions. *ChemElectroChem* **2020**, *7*, 2740-2751.
14. Faid, A. Y.; Barnett, A. O.; Seland, F.; Sunde, S., NiCu mixed metal oxide catalyst for alkaline hydrogen evolution in anion exchange membrane water electrolysis. *Electrochim. Acta* **2021**, *371*, 137837.
15. Guo, W.; Kim, J.; Kim, H.; Ahn, S. H., Direct electrodeposition of Ni-Co-S on carbon paper as an efficient cathode for anion exchange membrane water electrolyzers. *Int. J. Energy Res.* **2021**, *45* (2), 1918-1931.
16. Faid, A.; Oyarce Barnett, A.; Seland, F.; Sunde, S., Highly Active Nickel-Based Catalyst for Hydrogen Evolution in Anion Exchange Membrane Electrolysis. *Catalysts* **2018**, *8* (12), 614.
17. Park, Y. S.; Lee, J. H.; Jang, M. J.; Jeong, J.; Park, S. M.; Choi, W.-S.; Kim, Y.; Yang, J.; Choi, S. M., Co<sub>3</sub>S<sub>4</sub> nanosheets on Ni foam via electrodeposition with sulfurization as highly active electrocatalysts for anion exchange membrane electrolyzer. *Int. J. Hydrogen Energy* **2020**, *45* (1), 36-45.
18. Raja Sulaiman, R. R.; Wong, W. Y.; Loh, K. S., Recent developments on transition metal-based electrocatalysts for application in anion exchange membrane water electrolysis. *Int. J. Energy Res.* **2021**, *46* (3), 2241-2276.
19. Gallant, D.; Pézolet, M.; Simard, S., Optical and Physical Properties of Cobalt Oxide Films Electrogenerated in Bicarbonate Aqueous Media. *J. Phys. Chem. B* **2006**, *110*, 6871-6880.